Spatial distribution, temporal variation, and sources of heavy metal pollution in groundwater of a century-old nonferrous metal mining and smelting area in China

Xing Gong · Zhihua Chen · Zhaohui Luo

Abstract This study first presents the spatial distribution, temporal variation, and sources of heavy metal pollution in groundwater of a nonferrous metal mine area in China. Unconfined groundwater was polluted by Pb, Zn, As, and Cu, in order, while confined karst water in the mines showed pollution in the following sequence: Zn, Cd, Cu, Pb, and As. Pollution by Pb was widespread, while Zn, As, Cu, and Cd were found to be high in the north–central industrial region and to decrease gradually with distance from smelters and tailings. Vertically, more Pb, Zn, Cu, and Cd have accumulated in shallow Quaternary groundwater, while more As have migrated into the deeper fracture groundwater in the local discharge area. Zn, Cd, and Cu concentrations in groundwater along the riverside diminished owing to reduced wastewater drainage since 1977, while samples in the confluence area were found to have increasing contents of Pb, Zn, As, Cu, and Cd since industrialization began in the 1990s. Sources of heavy metals in groundwater were of anthropogenic origin except for Cr. Pb originated primarily from airborne volatile particulates, wastewater, and waste residues and deposited continuously, while Zn, Cd, and Cu were derived from the wastewater of smelters and leakage of tailings, which corresponded to the related soil and surface residue researches. Elevated As values around factories might be the result of chemical reactions. Flow patterns in different hydrogeological units and adsorption capability of from Quaternary sediments restricted their cross-border diffusion.

X. Gong
Graduate School, China University of Geosciences (Wuhan), No. 388, Lumo Road, Hongshan District, Wuhan 430074, People's Republic of China
e-mail: g_xing@126.com

Z. Chen (✉) · Z. Luo
School of Environmental Studies, China University of Geosciences (Wuhan), No. 388, Lumo Road, Hongshan District, Wuhan, Hubei 430074, People's Republic of China
e-mail: zhchen@cug.edu.cn

Z. Luo
e-mail: zhhluo@cug.edu.cn

Introduction

Since heavy metal toxicity has a lasting impact on natural ecosystems (Lee et al. 2013; Rai 2010) and human health (Bade et al. 2013; Maharia et al. 2010; Park and Lee 2013), a great deal of concern has been expressed over the problems of heavy metals in the environment. Anthropogenic activities such as mining and smelting bring much and various heavy metals into the ecosystem (Park and Choi 2013; Zhang and Zhao 1996; Zobrist et al. 2009). The study area located in Hunan Province of China has been known as an important lead (Pb), zinc (Zn), copper (Cu), and gold (Au) mining and smelting site for more than 110 years. Large amounts of toxic emissions released heavy metals, causing pollution in rivers (Li et al. 2011; Zhang et al. 2010),

soils (Li et al. 2012; Li et al. 2011), plants (Sun et al. 2012; Wang et al. 2008), river sediments (Sun et al. 2011), and animals (Zhang et al. 2013) during the long-term extensive industrialization.

The shallow groundwater in the area had been used widely for drinking until the 1990s and is exploited for irrigation, usually by hand-dug and/or drilled wells. As the drainage generated from mines, smelters, and ore-dressing plants flows to the land surface directly, pollutants can easily migrate into underlying aquifers. A comprehensive research on groundwater quality related to the geology, hydrology, geochemistry, pedology, meteorology, microbiology, and mining history (Salvarredy-Aranguren et al. 2008) is scarce in this area. The objective of this paper is to investigate the degree and distribution of heavy metal pollution in groundwater and to analyze its historical changes and sources.

Study area

The study area is located in southern Hunan Province. The climate is characterized by hot and wet periods in the summer and by cold and dry periods in the winter. The mean annual precipitation, most of which occurs in the spring and summer, is 1421.4 mm. The average annual temperature is 18.1 °C with northwestern prevailing winds. The study area is bounded by the easterly flowing Xiangjiang River in the north and Chonglingshui River in the east, a branch of Xiangjiang River, which flows from south to north. Two other smaller rivers, named Kangjiaxi and Zengjiaxia, cross the study area from south to north and joint the confluence of the Xiangjiang and Chonglingshui Rivers in the northeast as shown in Fig. 1.

The formations can be divided into six geologic units: (1) Quaternary sediments, (2) Cretaceous siltstone, (3) Jurassic sandstone, (4) granodiorite of early Yanshanian period (Ma et al. 2006), (5) mudstone and shale of Triassic and upper Permian, (6) carbonate rocks of bottom Permian, Carboniferous, and upper Devonian as reflected in the cross section of Fig. 1.

The Quaternary gravel and clay is about 10 m thick and contains a small amount of pore water (Q) recharged by precipitation. Fracture water in the Cretaceous siltstone (C) is found present in two groundwater flow systems (Cretaceous groundwater flow systems I and II) separated by a topographical watershed (Toth 1999) which is made up of sandstone and granodiorite. The

two systems flow to the Xiangjiang and Chonglingshui Rivers, respectively. Some fracture water is also found in superficial weathering fractures of the Jurassic sandstone (J). There is negligible groundwater in the deep dense sandstone which acts as the aquitard to separate the Jurassic groundwater flow system from others. The Permian, Carboniferous, and upper Devonian carbonate rocks are aquifers that contain karst water (K). They can also be further divided into three flow systems (Karst groundwater flow systems I, II, and III) due to the presence of impermeable mudstone and shale of Permian and Triassic ages between them, i.e., the S mine region, western region, and eastern region (including K mine) (Gong et al. 2013). The unconfined groundwater (Q, C, and J) has weak hydraulic connection to the confined karst water because of the aquiclude that is made up of mudstone, shale, and deep dense siltstone (Fig. 1).

The regional topography controls the groundwater flow pattern effectively. Since the topography declines from south to north, both fracture water of the two Cretaceous groundwater flow systems and karst water of the Karst groundwater flow system II move toward the Xiangjiang River from south to north. However, karst water of the eastern region (Karst groundwater flow system III) and S mine (Karst groundwater flow system I) drain to mining tunnels intensively, with depths of over 200 m in the mining area. Water of the Jurassic weathered fracture zone flows downhill and runs into rivers eventually. The Quaternary pore water near the rivers drains into the rivers directly. However, the confluence area between the Kangjiaxi and Zengjiaxi Rivers is the local discharge area for shallow pore water owing to its low lying position.

The local nonferrous metal operations are located in the north–central region with a number of production facilities in the study area, including third smelter (running since 1908), fourth smelter (running since 1952), sixth smelter (running since 1957), eighth smelter (running since 2005), K mine (exploiting Pb, Zn, and Au since 1992), S mine (exploiting Pb, Zn, and Cu since 1896), and other industries (Jinxin smelter, Dongsheng smelter). Two huge tailings of K mine and S mine lie along the Kangjiaxi and Zengjiaxi Rivers, respectively (Fig. 1). The mined rocks in the study area contain naturally produced Pb, Zn, Cu, and Au (Gao 1989; Sun et al. 2011), which may have dissolved into the groundwater spontaneously. However, anthropogenic heavy metals in high concentrations, i.e., Pb, Zn, As,
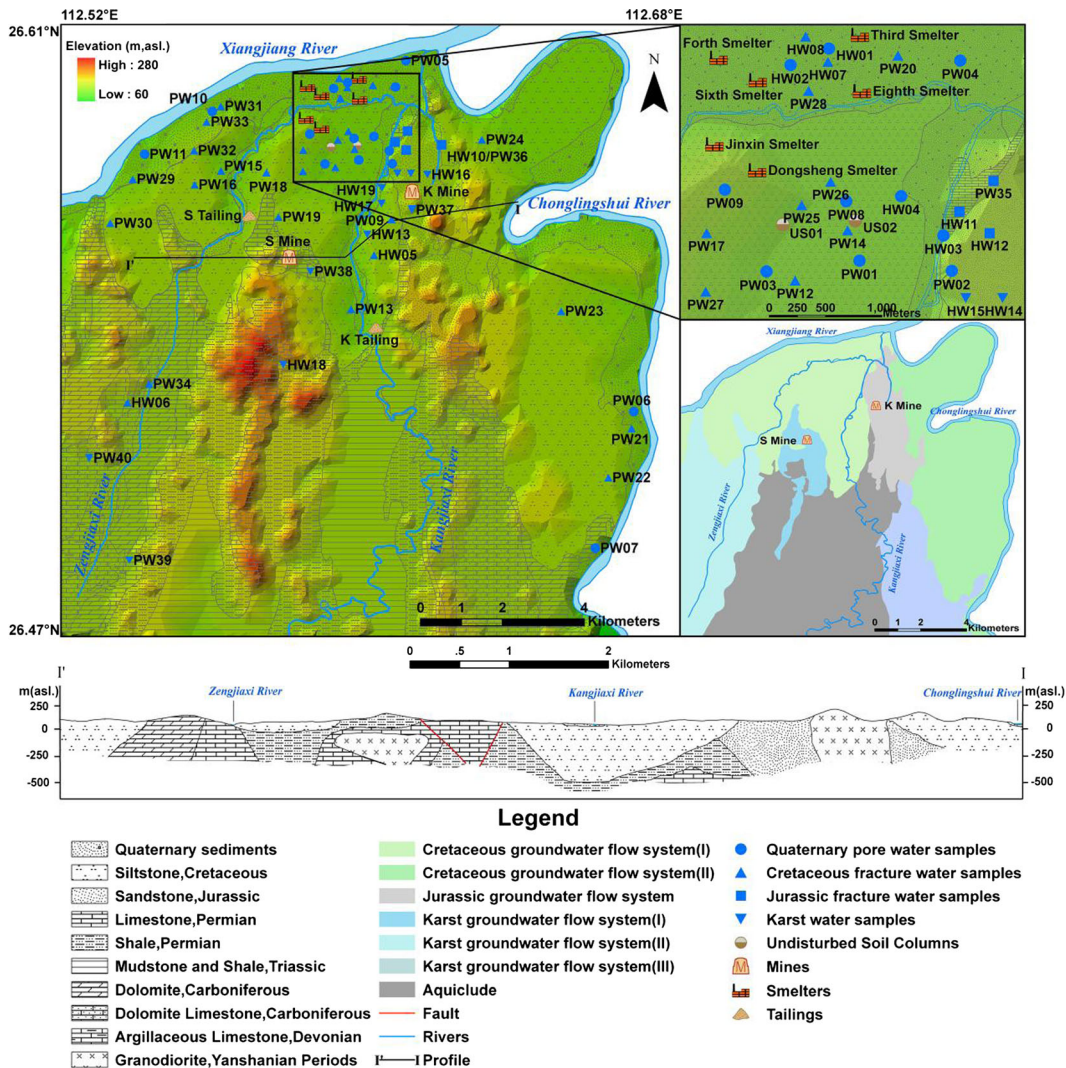
Fig. 1 Hydrogeological map of the study area with sampling points

Cd, Cu, and Hg, have migrated slowly from ground surface to groundwater in and around the industrial area (Sun et al. 2012).

Materials and methods

A total of 40 groundwater samples were collected from springs, wells, boreholes, and tunnels in September 2011, covering all groundwater types in the study area. Overall, there were 11 pore-water, 23 Cretaceous fracture water, 2 Jurassic fracture water, and 4 karst water samples. Two 500-ml pre-cleaned polyethylene bottles were used for water sample collection after rinsing twice with the water to be sampled prior to filling. Samples

were preserved with ultrapure HNO_3 to pH<2 for heavy metal analysis. The measurement of pH was made in the field using a pH meter (PHS-3C) of glass electrode method. Measurements and analyses were performed according to the standard procedures method by China's Environmental Protection Agency (SEPA 2002). The tested heavy metals included lead (Pb), zinc (Zn), arsenic (As), cadmium (Cd), copper (Cu), and chromium (Cr). The concentrations of heavy metals from the collected samples were tested at the Wuhan Center for Surveillance, Inspection and Testing of the Environment and Resources of China's Ministry of Land and Resources, using an inductively coupled plasma optical emission spectrometer (ICAP-6300). After calibrating the spectrometer by standard samples with an error of

less than 5 %, collected groundwater samples were measured with a standard sample validation every 10 tested samples and 2 parallel sample verification every 35 tested samples with the error of less than 5 %. In addition, 14 historical data of groundwater chemical analysis conducted between 1977 and 1991 were also obtained from the local nonferrous metals company.

In order to investigate the migration of heavy metals from land surface to groundwater, 12 undisturbed soil sections were sampled at different depths in two soil profiles of hydrogeological boreholes (US01 and US02). The boreholes are located at the shallow groundwater discharge area and close to factories in order to monitor the heavy metal pollution transportation and accumulation. Since the heavy metal pollutants migrated from surface to deep soil, six undisturbed sections each with a height of 20 cm and diameter of 110 mm were collected in US01 from top to bottom at depths of 0–0.2, 0.4–0.6, 0.8–1.0, 1.3–1.5, 1.7–2.0, and 3.0–3.2 m and another six in US02 at 0–0.2, 0.3–0.4, 0.5–0.6, 1.0–1.2, 1.5–1.6, and 4.8–5.0 m, which can be used to investigate the migration of heavy metals. Concentrations of lead (Pb), arsenic (As), cadmium (Cd), chromium (Cr), and copper (Cu) in soil sections and their leachates were analyzed by atomic fluorescence spectrometry (AFS-2202E) and flame atomic adsorption spectrometry (TAS-990). The leaching experiments were done according to the solid waste-extraction procedure for leaching toxicity-sulfuric acid and nitric method of the Chinese Industry Standard (SEPA 2007). Soil sections were soaked in the mixture of concentrated sulfuric acid and nitric acid with a pH of 3.20±0.05, and the solutions were oscillated with overturning oscillator in the speed of 30±2 r/min, then the leachates were extracted by using Zero-Headspace Extraction Vessel.

Results

Background values of heavy metals in groundwater

Heavy metals enter groundwater by two natural processes, geologic weathering and dissolution from soils and rocks (Haloi and Sarma 2012; Namaghi et al. 2011), and by anthropogenic inputs (Bakis and Tuncan 2011; Zamani et al. 2012). The study area is affected by the above two factors simultaneously (Sun et al. 2011). The historical data from 1977 to 1991 (Table 1) did not cover all heavy metals studied in 2011. Nevertheless, they can still be used for comparison to illustrate the natural background values of different groundwater types and then to assess the degree of anthropogenic inputs and pollution.

In terms of Quaternary pore water, the samples (HW01, HW02) collected near the Xiangjiang River were found to have increased concentrations of Pb, Zn, As, Cd, and Cu. The increase can be attributed to pollution by smelting activities of the third, fourth, and sixth smelters. On the other hand, those collected from exploration boreholes of K mine (HW03, HW04), further away from the smelters, showed only smaller increases in Zn values. Because the background values of Pb, As, and Cu and pH in north Hunan Province were similar to those in HW03 and HW04 (Lian and Xiao 2010), they were accepted as background values for pore water (Table 1).

Similarly, Cretaceous fracture water samples collected in 1977 were typically acidic and of higher concentration in Pb, Zn, As, and Cu. The drinking water sample (HW05) located far away from smelters was slightly alkaline and showed decreasing values of Pb, As, and Cu, while the values of As, Cr, and pH were similar to those of HW09 that collected from the borehole of K mine before the mineral exploitation. Consequently, historical data of HW5 can be considered as background values for Cretaceous fracture water (Table 1).

Jurassic fracture water samples between 1978 and 1986 showed slight differences, with neutral pH, and minimal changes in Pb, As, Cr, and Cu and little Zn. Heavy metal concentrations were also close to background values of north Hunan Province. Values of spring water (HW10) were used as background values (Table 1).

The karst aquifers of K mine are of Permian limestone, with higher contents of Pb and As but lower in Zn than the average contents in the Earth's crust and the Jurassic sandstone of the study area (Tan and Wang 2008). The karst water samples of K mine thus had more Pb and As but less Zn than water samples of north Hunan Province and the Jurassic fracture water (Table 1). Because the karst water has weak hydraulic connection with unconfined groundwater, the samples collected before mining activities were almost natural, for instance, the Longwang Spring. Consequently, the average values of the historical data have been taken as background values for the karst water (Table 1).

Table 1 Historical and background values of heavy metal concentrations and pH in groundwater

No.	Sampling types	Sampling date	Heavy metals concentrations (mg L^{-1})						pH
			Pb	Zn	As	Cd	Cr	Cu	
Quaternary pore water									
HW01	Borehole	April 1977	0.0140	0.4400	–	0.0050	–	0.0500	6.40
HW02	Borehole	April 1977	0.0350	0.4000	0.0400	0.0100	–	0.0200	6.40
HW03	Borehole	Sep 1981	0.0020	0.3900	<0.0020	–	–	<0.0020	6.80
HW04	Borehole	Sep 1981	<0.0020	0.0620	<0.0020	–	–	<0.0020	6.80
Background values									
North Hunan Province [a]			0.0005	0.0140	0.0010	0.0031	0.0010	0.0010	6.74
Study area			0.0005	0.0140	0.0010	0.0031	0.0010	0.0010	6.74
Cretaceous fracture water									
HW05	Well	Sep 1978	–	–	–	–	–	–	7.42
		Sep 1981	<0.0020	0.0100	<0.0020	<0.0010	–	<0.0020	7.20
HW06	Spring	Sep 1978	–	–	–	–	–	–	7.27
HW07	Borehole	April 1977	0.0020	0.0280	0.0100	0.0400	–	0.0230	6.40
HW08	Borehole	April 1977	0.0044	0.0800	–	0.0100	–	0.0240	6.42
HW09	Borehole	Oct 1986	–	–	0.0020	–	<0.0010	–	6.91
Background values									
North Hunan Province [a]			0.0010	0.0171	0.0012	0.0052	0	0.0010	6.39
Study area			<0.0020[c]	0.0100	<0.0020	<0.0010	<0.0010	<0.0020	7.20
Jurassic fracture water									
HW10	Spring	Sep 1978	–	–	–	–	–	–	7.17
		Sep 1981	<0.0020	0.0112	<0.0020	<0.0010	–	<0.0020	6.95
		Oct 1986	–	–	0.0010	–	<0.0010	–	7.22
HW11	Borehole	Sep 1981	<0.0020	0.0820	<0.0020	–	–	<0.0020	6.90
HW12	Tunnel	Oct 1986	–	–	0.0040	–	<0.0010	–	7.96
Background values									
North Hunan Province			0.0005	0.0135	0.0015	0.0016	0	0.0010	6.75
Study area			<0.0020	0.0112	0.0010	<0.0010	<0.0010	<0.0020	7.11
Karst water[b]									
HW13	Borehole	Sep 1978	–	–	–	–	–	–	7.97
HW14	Flank hole	July 1985	0.0140	0.0143	–	–	<0.0010	–	7.65
		Dec 1986	0.0170	0.0190	0.0080	<0.0010	<0.0040	<0.0020	7.91
HW15	Drainage hole	Oct 1986	–	–	0.0020	–	<0.0010	–	7.47
		Dec 1986	0.0160	0.0150	0.0120	<0.0010	<0.0040	<0.0020	7.85
HW16	Drainage hole	Oct 1986	–	–	0.0040	–	<0.0010	–	7.42
		Dec 1986	0.0170	0.0170	0.0080	<0.0010	<0.0040	<0.0020	7.83
HW17	Borehole	Dec 1986	0.0110	0.0150	0.0060	<0.0010	<0.0040	<0.0020	7.87
		Sep 1987	–	–	–	–	<0.0010	–	7.00
HW18	Spring	July 1986	–	–	0.0080	<0.0010	–	–	7.37
HW19	Borehole	Sep.1987	–	–	–	–	<0.0010	–	7.10
		June 1991	–	–	0.0020	–	–	–	7.34
Background values									
North Hunan Province			0	0.1470	0.0024	0	–	0.0010	7.05
Study area			0.0150	0.0161	0.0063	<0.0010	<0.0010	<0.0020	7.57

[a] Background values of groundwater in north Hunan Province according to Lian and Xiao 2010

[b] Karst water samples were collected from boreholes, flank holes, drainage holes of K mine and Longwang Spring

[c] Lower than the detection limit of which half values were used for EFs calculation and multivariate statistical analysis

Heavy metal pollution in groundwater

Average concentrations of Pb, Zn, As, Cd, Cr, and Cu in groundwater were 0.0843, 0.1665, 0.0051, 0.0014, 0.0010, and 0.0018 mg/L, respectively (Table 2). In terms of drinking water requirements (WHO 2011), all the samples were disqualified because of excessive Pb (higher than 0.0100 mg/L) and only the karst water in S mine had too much Zn (Fig. 3b). In addition, the Cretaceous fracture water samples around smelters and the karst water of K mine had disqualified As, while the Quaternary pore water near smelters and the karst water in K mine had excessive Cd (Fig. 3d). Concentrations of Cu and Cr were acceptable in all samples. Twenty percent of pH values of groundwater samples were lower than 6.5, occurring in Quaternary pore water and Cretaceous fracture water along the rivers only (Fig. 3g).

Enrichment factors (EFs) were used to evaluate the degree of pollution by comparing background values to present concentrations of heavy metals in this study:

$$\mathrm{EF}_i^j = \frac{C_i^j / C_i^{\mathrm{cr}}}{C_k^j / C_k^{\mathrm{cr}}}(i = 1, 2, \ldots\ldots, 40; j = \mathrm{Pb, \ Zn, \ As, \ Cd, \ Cu}; \ k = \text{groundwater types})$$

EF_i^j Enrichment factors of element j of sample i in 2011

C_i^j Concentration of element j of sample i in 2011

C_i^{cr} Cr concentration of sample i in 2011

C_k^j Background value of element j of groundwater water type k

C_k^{cr} Background value of Cr of groundwater water type k.

Cr was the only element without temporal variation as compared to background values (Table 2). It distributed randomly in all groundwater types, likely to be irrelevant to heavy metal emissions (Fig. 3f). Also, it has limited human disturbance (Hernandez et al. 2003) and temporal fluctuation (Schiff and Weisberg 1999). Consequently, it was taken as the conservative element as other earlier studies (Huntsman-Mapila et al. 2005; McMurtry et al. 1995). A range between 0.5 and 2 of EFs represented the normal variation, while a value higher than 2 showed anthropogenic pollution (Hernandez et al. 2003; Sutherland 2000).

Quaternary pore water was found to contain elevated values of Pb, Zn, As, and Cu with average EFs of 282.58, 15.31, 2.95, and 2.13, respectively. These values represent anthropogenic enrichments, except for the EFs of Cd which indicate little pollution (Fig. 2). Samples with elevated Pb concentrations are present everywhere in the study area, with the highest values close to smelters and mines (Fig. 3a). The distributions of Zn and Cu were similar, accumulating more in the north region along the Xiangjiang River (Fig. 3b, e), while As and Cd were more concentrated at the confluence area of Kangjiaxi and Zengjiaxi Rivers (Fig. 3c, d).

The samples of lower pH values along rivers were contaminated by acid drainage from smelters and tailings driven by the topography controlled water table.

Pb and Zn concentrations were found to be higher in most Cretaceous fracture water samples than background values (Table 2). Pb pollution with the largest excessive EFs (average of 55.64, Fig. 2a) was widespread and similar to that in the Quaternary pore water (Fig. 3a). By contrast, most EFs of Zn (average of 2.51) indicated slight contamination (Fig. 2b), and Cu in Cretaceous fracture water did not show any anthropogenic pollution with an average EF of 0.76 (Fig. 2e), except for a few samples along the Xiangjiang River (Fig. 3e). However, 52.17 % of samples had higher As values than the background with an average EF of 6.63 (Fig. 2c), which occurred at the confluence area. These samples contained more As than Quaternary pore water samples (Fig. 3c), which was the opposite in the case of Pb, Zn, and Cu. Cretaceous water samples showed trace amounts of Cd (Table 2), suggesting negligible anthropogenic pollution with an average EF of 0.64 (Fig. 2d). The acid samples were located near smelters and tailing which discharged acid wastewater (Fig. 3g).

Groundwater in weathered fractures of the Jurassic sandstone contained more Pb than background values, with an average EF of 13.16 (Fig. 2a), obviously indicating anthropogenic inputs. Fortunately, Zn and As concentrations of Jurassic springs are only slightly elevated with normal values varying between EFs of 0.51 and 0.61, respectively (Fig. 2b, c). Jurassic fracture water contained minimal Cd and Cu, similar to historical data, which is also true for the pH values (Table 2).

Table 2 Heavy metal concentrations and pH of groundwater samples in the study area

No.	Sampling type/depth (m)	Heave metals concentrations (mg L^{-1})						pH
		Pb	Zn	As	Cd	Cr	Cu	
Quaternary pore water (Q)								
Background values		0.0005	0.0140	0.0010	0.0031	0.0010	0.0010	6.74
PW01	Well/6	0.0508	0.0792	0.0009	0.0015	0.0009	0.0016	6.95
PW02	Well/6	0.0215	0.3989	<dl	0.0026	<dl	0.0006	6.27
PW03	Well/8	0.0825	0.2722	0.0014	0.0037	<dl	0.0024	6.75
PW04	Well/10	0.2313	0.1935	0.0065	0.0042	0.0050	0.0074	5.30
PW05	Well/14	0.3652	0.0883	0.0018	<dl	0.0012	0.0038	6.06
PW06	Well/8	0.0623	0.0552	<dl	<dl	0.0013	0.0017	6.87
PW07	Well/15	0.0295	0.0131	0.0044	<dl	0.0018	0.0006	7.25
PW08	Well/11	0.3523	0.3285	0.0065	0.0069	0.0010	0.0033	7.25
PW09	Well/15	0.0949	0.0552	0.0048	0.0006	<dl	<dl	6.83
PW10	Well/11	0.1010	0.0713	<dl	0.0008	0.0010	0.0014	5.56
PW11	Well/12	0.0844	0.0426	0.0019	<dl	<dl	0.0015	5.40
Cretaceous fracture water (C)								
Background values		<0.0020[c]	0.0100	<0.0020	<0.0010	<0.0010	<0.0020	7.20
PW12	Well/40	0.0420	0.0261	0.0070	<dl	<dl	<dl	7.24
PW13	Well/33	0.0566	0.0356	0.0012	<dl	0.0012	<dl	6.21
PW14	Well/30	0.0937	0.0213	0.0216	0.0006	<dl	0.0006	7.43
PW15	Well/30	0.0650	0.0375	<dl	<dl	0.0015	<dl	7.42
PW16	Well/25	0.0789	0.0118	0.0019	<dl	0.0038	0.0010	6.68
PW17	Well/45	0.0634	0.0336	0.0025	<dl	<dl	<dl	6.67
PW18	Well/18	0.0339	0.0223	0.0043	<dl	<dl	<dl	6.84
PW19	Well/30	0.0775	0.0164	<dl	<dl	<dl	<dl	7.40
PW20	Spring/0.1	0.1096	0.0198	0.0155	0.0011	<dl	0.0023	7.21
PW21	Well/60	0.0564	0.0244	<dl	<dl	<dl	<dl	6.70
PW22	Spring/0.1	0.0169	<dl	0.0009	<dl	<dl	<dl	7.06
PW23	Well/40	0.0588	0.0188	0.0078	<dl	<dl	<dl	7.20
PW24	Well/44	0.0394	0.0258	<dl	<dl	0.0028	<dl	6.78
PW25	Well/40	0.0278	0.0164	0.0364	<dl	<dl	<dl	7.40
PW26	Well/20	0.0731	0.0218	0.0130	<dl	<dl	<dl	7.07
PW27	Well/20	0.0948	0.0552	0.0055	<dl	<dl	0.0013	6.92
PW28	Well/35	0.0512	0.0464	0.0189	<dl	<dl	0.0021	6.75
PW29	Well/52	0.0679	0.0302	<dl	<dl	<dl	<dl	7.16
PW30	Well/40	0.0196	0.0368	<dl	<dl	0.0021	<dl	7.29
PW31	Well/50	0.0774	0.0400	<dl	<dl	<dl	0.0018	5.60
PW32	Well/70	0.0391	0.0117	<dl	<dl	0.0033	0.0006	7.40
PW33	Well/14	0.0514	0.0338	<dl	<dl	<dl	0.0038	6.24
PW34	Well/10	0.0900	0.0532	<dl	<dl	<dl	<dl	7.46
Jurassic fracture water (J)								
Background values		<0.0020	0.0112	0.0010	<0.0010	<0.0010	<0.0020	7.11
PW35	Spring/0.1	0.0408	0.0154	0.0025	<dl	0.0016	<dl	6.93
PW36	Spring/0.1	0.0434	0.0208	0.0014	<dl	0.0016	<dl	7.28
Karst water (K)								

Table 2 (continued)

No.	Sampling type/depth (m)	Heave metals concentrations (mg L^{-1})						pH
		Pb	Zn	As	Cd	Cr	Cu	
Background values		0.0150	0.0161	0.0063	<0.0010	<0.0010	<0.0020	7.57
PW37	Tunnel/475	0.0612	0.1593	0.0253	0.0049	<dl	0.0030	7.45
PW38	Tunnel/510	0.2622	4.1720	0.0034	0.0206	<dl	0.0254	7.39
PW39	Well/16	0.0637	0.0354	0.0017	<dl	<dl	<dl	8.07
PW40	Well/50	0.0412	0.0211	<dl	<dl	<dl	0.0007	7.51

<dl: lower than the detection limit for Pb (0.0024 mg/L), Zn (0.0012 mg/L), As (0.0009 mg/L), Cd (0.0006 mg/L), Cr (0.0009 mg/L), and Cu (0.0006 mg/L); half values of them were used for EFs calculation and multivariate statistical analysis

The situation of karst water can be explained in terms of hydrogeological units. Because of low ore content, As, Cd, Cr, and Cu concentrations of samples in the western region (karst groundwater flow system II) were even lower than the historical data of K mine, while Zn values were only slightly elevated. But the samples also showed Pb pollution similar to that in other groundwater types (Fig. 3a), with EFs of 4.72 for PW39 and 3.05 for PW40. By contrast, heavy metal concentrations of samples in the mining area (PW37, PW38) were much higher than the background values (Table 2), demonstrating serious Pb, Zn, Ad, Cd, and Cu pollution with average EFs of 11.98, 149.46, 2.53, 28.33, and 15.78, respectively. Moreover, the quality of karst water in S mine was worse than that in K mine, owing to longer mining activities. The pH of karst water remained slightly alkaline as in the past (Fig. 3g), likely resulting from

the water interaction with limestone in the aquifer, indicating that the karst water was isolated from the acid unconfined groundwater and smelting drainage.

In general, Quaternary pore water has shown the most heavy metal pollution, followed by Cretaceous fracture water, karst water, and Jurassic fracture water. Pb was the most polluting element in different groundwater except for the buried karst water in mines, preceding Zn, As, Cu, and Cd overall. The pollution degree in the karst water of the mining area was, in decreasing order, Zn, Pb, Cd, Cu, and As.

Regarding the spatial distribution of the above elements, Pb was spread over the study area uniformly. Elevated concentrations of Zn, As, Cd, and Cu occurred in the proximity of smelters and mines, decreasing gradually with increasing distance from processing plants. The distributions of Zn, Cd, and Cu were similar,
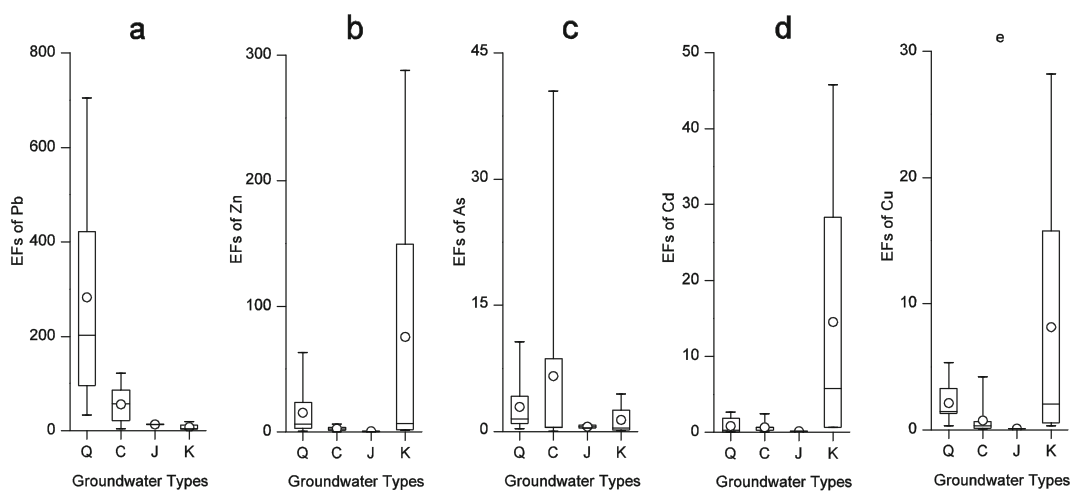

Fig. 2 EFs of Pb, Zn, As, Cd, and Cu in different groundwater types (minimum, 25, 50, and 75 % quartiles; maximum values in *lines* from bottom to top and average values in *circle*; Q, C, J, and K represent Quaternary pore water, Cretaceous fracture water, Jurassic fracture water, and Karst water samples, respectively)
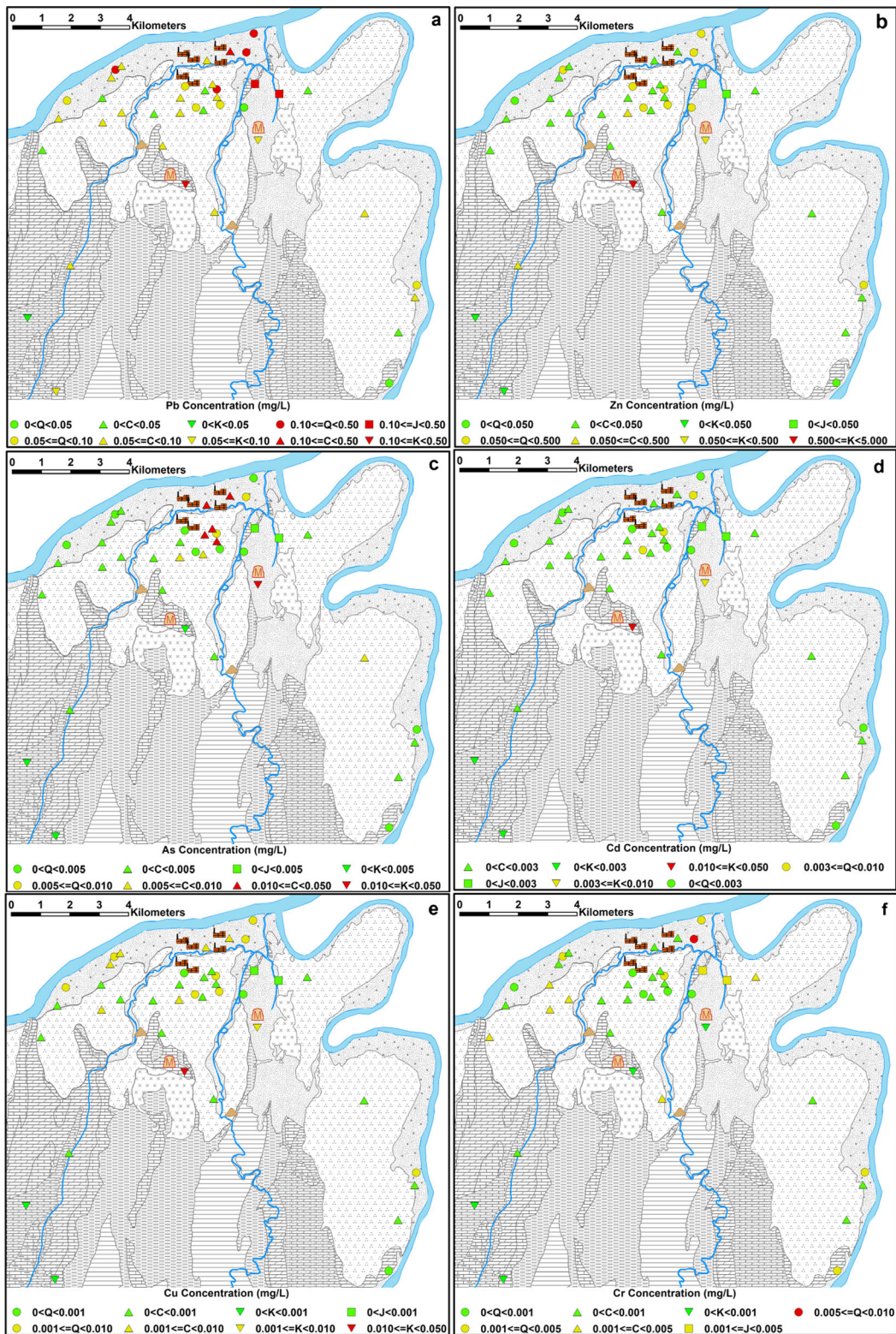
Fig. 3 Spatial distribution of heavy metal concentrations and pH in groundwater (*circles*, *upward triangles*, *downward triangles*, and *squares* represent Quaternary pore water (*Q*), Cretaceous fracture water (*C*), Jurassic fracture water (*J*), and Karst water (*K*) samples, respectively)
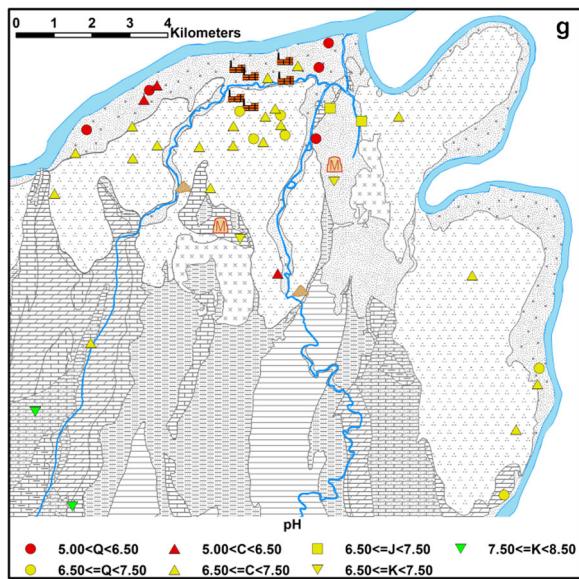
Fig. 3 (continued)

concentrations in groundwater over the past four decades could be shown by comparing historical values with present concentrations. Based on the reliability of historical data as well as on distances between sampling positions, nine pairs of historical and present groundwater samples were compared with each other. The temporal variations of pollution in groundwater were different in corresponding groundwater types and hydrogeological units (Fig. 4).

Samples collected along Xiangjiang River in 2011 were found with less Zn, Cd, and Cu but more Pb than those of 1977 (Fig. 4a). The decrease of Zn, Cd, and Cu was the result of the reduction of smelting wastewater that occurred from the improvement of wastewater treatment and implementation of environmental laws and regulations. The increased Pb may come from other airborne sources which spread more readily. However, the case of As was different, namely, decreasing in Quaternary pore water (pair 1) but increasing in Cretaceous fracture water (pairs 2 and 3) from 1977 to 2011, thus demonstrating different sources or factors that impact its migration.

Since the commissioning of the eight, Jinxin, and Dongsheng smelters after the 1990s, the quality of groundwater at the confluence area of Kangjiaxi River and Zengjiaxi River has clearly deteriorated (Fig. 4b). Pb concentrations in groundwater increased greater than 10 times. In addition, concentrations of Zn, As, and Cu were much higher than corresponding past values. Cd concentration of PW08 exceeded the background value, indicating anthropogenic input. Specifically, the Quaternary pore water sample located close to smelters (PW08) showed a larger increase in heavy metals than
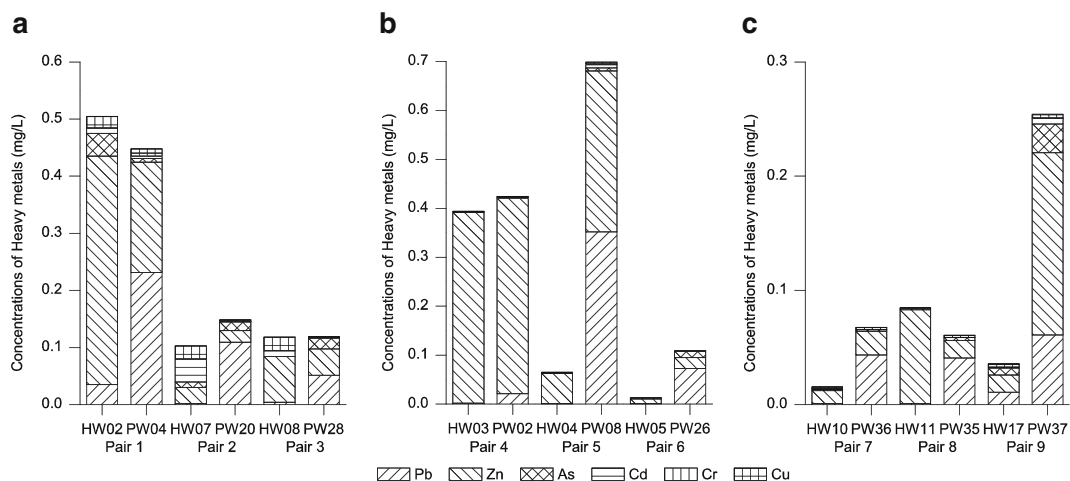
Temporal variation of heavy metal pollution in groundwater

Since historical sampling locations were close to some of the 2011 sampling sites, variation in heavy metal

attenuating from shallow aquifers to deep aquifers, while As tended to concentrate more in deeper fracture water at the confluence area of Kangjiaxi and Zengjiaxi Rivers.

Fig. 4 Concentrations of heavy metals in groundwater pair samples from 1977 to 2011 (**a–c** represent subregions of sample collecting)
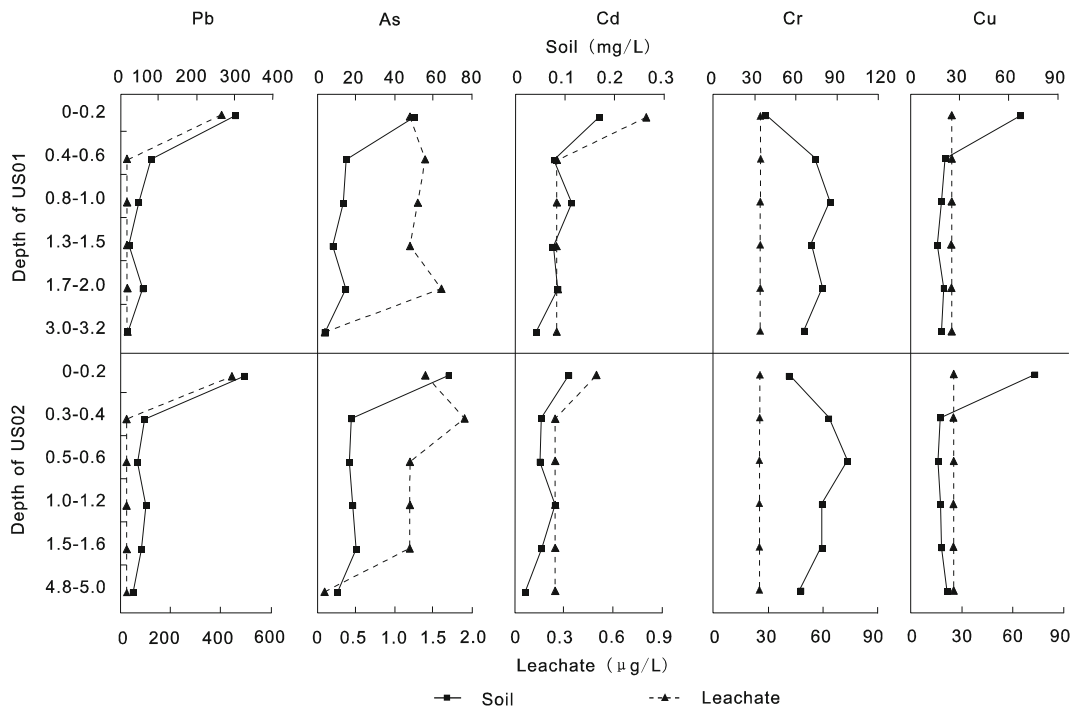
Fig. 5 Heavy metal concentrations in soil and leachate profiles

the one far away (PW02), illustrating that the pollutant originates to a large degree from smelters. Similar to the north region along Xiangjiang River, more As accumulated in Cretaceous fracture water (PW08), while the other elements have concentrated more in nearby Quaternary pore water (PW26).
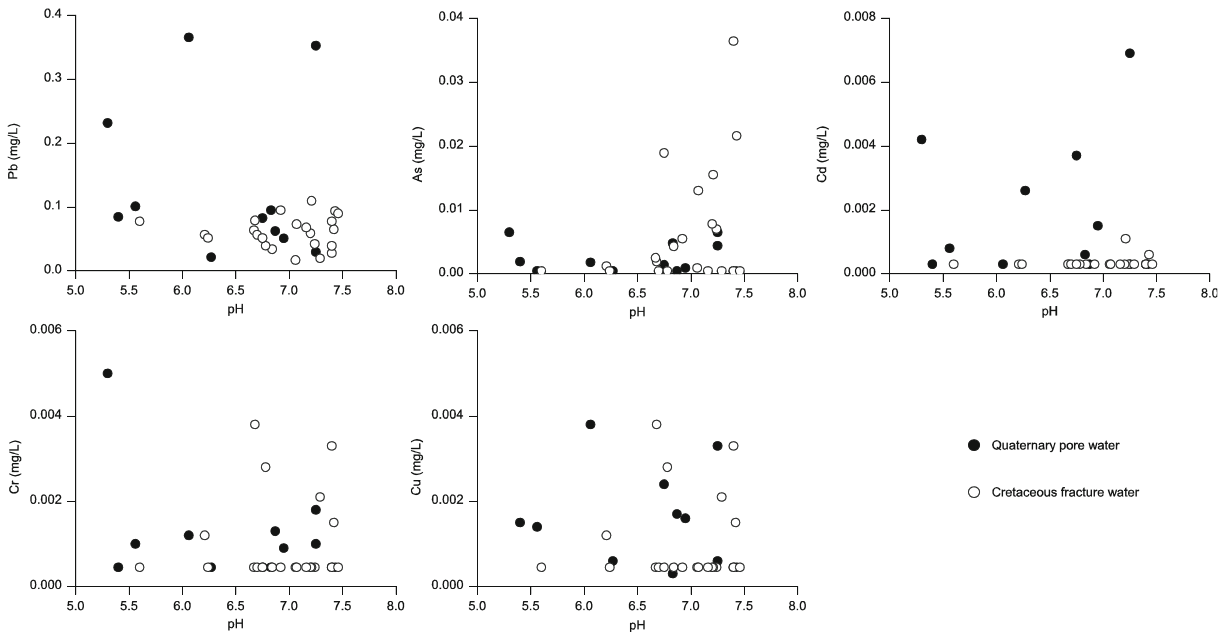

Fig. 6 Concentrations of Pb, As, Cd, Cr, and Cu and pH in Quaternary pore water and Cretaceous fracture water

Table 3 Correlations between heavy metals in groundwater

	Pb	Zn	As	Cd	Cr	Cu
Pb	1					
Zn	0.411*	1				
As	−0.017	−0.038	1			
Cd	0.533*	0.943*	0.051	1		
Cr	0.133	−0.087	−0.193	−0.026	1	
Cu	0.551*	0.949*	0.003	0.936*	0.043	1

*p=0.01 (correlation is significant (two-tailed))

Jurassic Springs (pairs 7 and 8) revealed a significant increase in Pb but little changes in Zn, As, Cd, and Cu from 1981 to 2011 (Fig. 4c). This indicates that at high altitudes Pb can infiltrate into groundwater by airborne transmission. Meanwhile, concentrations of Pb, Zn, As, Cd, and Cu in the karst water of K mine (pair 9) rose remarkably after exploitation of the ore began. It is clear that the karst water has been polluted by mining activities during the past 27 years.

Migration of heavy metals in soil profiles

Because the heavy metal concentrations in groundwater were much higher around processing plants, soil profiles collected in the industrial region were used to analyze the presence and velocity of heavy metal infiltration from the surface to the groundwater table. The trends of heavy metal concentrations varying with depth in soil and leachates profiles were generally comparable (Fig. 5). Concentrations of Cu and Cr in all leachates were lower than the detection limit, which was the same with concentrations of Pb and Cd in leachates deeper

Table 4 Rotated component matrix for principal component analysis loadings for heavy metals in groundwater

	PC1	PC2	PC3	PC4
Pb	0.323	0.943	0.078	−0.006
Zn	0.983	0.102	−0.076	−0.048
As	0.002	−0.004	−0.097	0.995
Cd	0.948	0.244	−0.014	0.051
Cr	−0.025	0.066	0.993	−0.098
Cu	0.949	0.257	0.053	0.007

Rotation method: Varimax with Kaiser Normalization

than 0.2 m. That is the reason for the constant values in Fig. 5.

As the severest polluting element in groundwater, Pb concentrations were highest in surface soils (depth of 0–0.2 m), agreeing with conclusions from previous investigations in the study area (Li et al. 2012; Wei et al. 2009). By contrast, surface soils accumulated less As, Cu, Cd, and Cr, which coincided with the chemical concentrations in groundwater, indicating that heavy metals in soils were able to infiltrate into groundwater.

Concentrations of Pb, As, Cu, and Cd decreased sharply at 0.2–0.4 m and declined slowly with depth, indicating the effective adsorption capability of the topsoil. However, the value of Cr in soils increased constantly from 0.2 to 0.6 m and remained stable at greater depths, which matched the equivalent concentrations in Quaternary pore water, Cretaceous fracture water, and even Jurassic fracture water (Fig. 6), thus suggesting native origins.

Heavy metal concentrations in leachates of corresponding soil sections were much lower than those in soils. Changes in Pb and Cd in leachates were similar to those of soils, decreasing dramatically from surface to depths of 0.4 m and maintaining minimal levels in deeper leachates. This indicates that Pb, Cd, and Cu in Quaternary sediments were difficult to dissolve and that they migrated into the groundwater vertically. Consequently, concentrations of Pb, Cd, and Cu in pore water are higher than those of Cretaceous fracture water (Fig. 6). However, As values in leachates showed an opposite trend to that of soils, namely, increasing from the surface to depths of 0.4 m and maintaining stability at 1.2 μg/L. In conclusion, As was easier to release from soil into groundwater during the dissolution and infiltration processes, which is supported by higher As concentrations in Cretaceous fracture water (Fig. 6).

Discussion

The heavy metals' spatial distribution illustrates that the smelting and mining activities were primarily responsible for the pollution of groundwater. Contaminants consisted of airborne volatile particulates released by large chimneys, wastewater of smelting and mineral processes, and leakage from tailings and waste residues of mineral processes. Specifically, the major pollutants in airborne volatile particulates are Pb and As, the wastewater contain H_2SO_4, Pb, Zn, As, Cd, and Cu,

and the waste tailings as well as residues contain Pb, Cu, and Zn primarily.

Correlation calculation and principal component analysis (PCA) were performed to explore for pollution sources of the above heavy metals (Panda et al. 2010), and 98.5 % of the variance could be explained when four principal components were considered (Tables 3 and 4). The results showed that Zn, Cd, and Cu correlated with one another closely and appeared in the first component. This suggests common sources of these elements (Al-Hobaib et al. 2013). Taking their similar spatial and temporal variation in groundwater and concentration soil and leachate profiles into account, one could ascertain that major sources of Zn, Cd, and Cu in unconfined groundwater and soils were wastewater of smelting and mineral processes. A similar situation is known in south Morocco (El Khalil et al. 2008). Elevated values of Cu and Zn were found downstream of the S tailing, driven from leakage of tailing, which corresponded to the Cu pollutions in the soil in the study area (Sun et al. 2012; Wei et al. 2009).

Since Pb showed positive correlation with Cd and Cu, but preformed as the second component alone, its sources may be complex as the various emissions. Firstly, widespread elevated Pb values in groundwater indicate that the Pb was derived from airborne volatile particulates transported via the prevailing northerly wind (Wei et al. 2009). But much higher concentrations of Pb around smelters and mines might be the result of acid wastewater and waste residues (Qiao et al. 2013).

Arsenic, with various free and/or non-free ions forms in groundwater, is an element of complicated geochemical properties (Acharyya et al. 2000; Flores and Rubio 2010; Horneman et al. 2004; Van Geen et al. 2004). The distribution of As in groundwater as well as its concentration profile in soils were similar to those of Zn and Cd, but they shared different characteristics in leachates and groundwater. Meanwhile, the negative correlation with others (Table 3), and a unique component, PC4 (Table 4), indicated some independent source(s) for As in groundwater.

Galena (PbS), sphalerite (ZnS), chalcopyrite (CuFeS2), and arsenopyrite (FeAsS) are the primary metal-bearing minerals in the study area (Zeng et al. 2000). Therefore, the reductive dissolution of iron oxide, e.g., Fe (Campbell et al. 2006; Islam et al. 2004; Tufano et al. 2008; Van Geen et al. 2004), might promote the release of As from the polluted soil into groundwater. After that, sorbed humic substances in

soils might accelerate the migration of As in groundwater (Murphy and Zachara 1995). Furthermore, the acid wastewater (Mok et al. 1988) as well as stagnant groundwater (Brown et al. 2007) could facilitate accumulation of As in the confluence area of the Kangjiaxi and Zengjiaxi Rivers. Thus, the highly concentrated As in unconfined groundwater might be the result of the chemical reaction between arsenic compounds in soils that were derived from airborne volatile particles (Wei et al. 2009) and acid groundwater with microbes (Islam et al. 2004; Oremland and Stolz 2003) during the leaching and infiltrating processes. However, As may also be released by other geochemical processes; the accurate sources and processes should be analyzed with more soil mineralogy, biological and physical chemistry, and geochemical condition data.

Cr showed negative correlation with others (Table 3) and appeared to be the unique rotated component (Table 4), suggesting independent sources unlike the above elements. Randomly distributed elevated Cr concentrations remained stable in all kinds of groundwater during the last 40 years, and the Cr concentrations in soils did not decrease with depth. This indicates a natural source in groundwater which was derived from parent materials (Wei et al. 2009).

However, because of the impermeable mudstone and shale above the limestone in the mining area, the confined karst water in the mines was polluted by Pb, Zn, As, Cd, and Cu which were dispersed from metal ore produced from mining activities.

More importantly, although the heavy metal pollution was critical, flow patterns in the different hydrogeological units restricted their cross-border diffusion. To be more specific, the regional groundwater that flowed from south to north limited heavy metals spreading from north to south. The groundwater close to the Xiangjiang River interacts with the river frequently, which has also contributed to the decline of Zn, As, Cd, and Cu concentrations in the northern region. The separation of the two Cretaceous groundwater flow systems protects the fracture water in the eastern region from pollution in the western region. Impermeable mudstone and shale isolated the southern karst water from the pollution of the mining regions. Similarly, heavy metal concentrations, except As and Cr in Quaternary pore water, were much higher than those in Cretaceous fracture water because of weak permeability and significant adsorption ability of Quaternary sediments. The recharge area of Jurassic fracture water, thickly overlain

by the alluvial deposit of sandstone with poor infiltration, received less pollutant and protected the groundwater from toxicities.

Conclusion

Groundwater in the study area was found to be polluted by Pb, Zn, As, Cd, and Cu due to smelting, mineral processing, and mining activities. Relative to background values, results show higher concentrations of heavy metals in the Quaternary pore water followed by Cretaceous fracture water, karst water, and Jurassic fracture water. Pb, the major contaminant in unconfined groundwater, is derived from airborne volatile particulates and wastewater of smelters and is increasing most rapidly and spreading most widely since 1977. Meanwhile, the wastewater of smelters and leakage of tailings and waste residues has lead to elevated Zn, Cd, and Cu in unconfined groundwater in the northern industrial region. Greater concentrations of As in the north–central area may come from the chemical reactions between anthropogenic arsenic compounds that were accumulated in the soil and acid groundwater impacted by wastewater and leakage. By contrast, randomly distributed Cr has a natural geologic source. The results highly corresponded with the recent soil and waste residues study. The hydrogeological conditions have restricted the diffusion of heavy metals in groundwater effectively. The first research for groundwater heavy metal pollution show significant contribution to local heavy metal migration and treatment study.

References

Acharyya, S. K., Lahiri, S., Raymahashay, B. C., et al. (2000). Arsenic toxicity of groundwater in parts of the Bengal Basin in India and Bangladesh: the role of quaternary stratigraphy and Holocene sea-level fluctuation. *Environmental Geology, 39*(10), 1127–1137.

Al-Hobaib, A. S., Al-Jaseem, Q. K., Baioumy, H. M., et al. (2013). Heavy metals concentrations and usability of groundwater at Mahd Adh Dhahab gold mine, Saudi Arabia. *Arabian Journal of Geosciences, 6*(1), 259–270.

Bade, R., Oh, S., Shin, W. S., et al. (2013). Human health risk assessment of soils contaminated with metal(loid)s by using DGT uptake: a case study of a former Korean metal refinery site. *Human and Ecological Risk Assessment, 19*(3), 767–777.

Bakis, R., & Tuncan, A. (2011). An investigation of heavy metal and migration through groundwater from the landfill area of Eskisehir in Turkey. *Environmental Monitoring and Assessment, 176*(1–4), 87–98.

Brown, B. V., Valett, H. M., & Schreiber, M. E. (2007). Arsenic transport in groundwater, surface water, and the hyporheic zone of a mine-influenced stream-aquifer system. *Water Resources Research, 43*(11).

Campbell, K. M., Malasarn, D., Saltikov, C. W., et al. (2006). Simultaneous microbial reduction of iron(III) and arsenic(V) in suspensions of hydrous ferric oxide. *Environmental Science & Technology, 40*(19), 5950–5955.

El Khalil, H., El Hamiani, O., Bitton, G., et al. (2008). Heavy metal contamination from mining sites in south Morocco: monitoring metal content and toxicity of soil runoff and groundwater. *Environmental Monitoring and Assessment, 136*(1–3), 147–160.

Flores, A. N., & Rubio, L. M. D. (2010). Arsenic and metal mobility from Au mine tailings in Rodalquilar (Almeria, SE Spain). *Environmental Earth Sciences, 60*(1), 121–138.

Gao, X. D. (1989). Geological characters of Shuikoushan gold deposit, Hunan Province. *Mineral Resources and Geology, 3*(12), 22–25.

Gong, X., Chen, Z. H., & Chen, Y. M. (2013). Discussion of metallurgical construction project groundwater environment impact assessment method. *Journal of Hunan University of Science & Technology (Natural Science Edition) (in Chinese), 28*(1), 102–108.

Haloi, N., & Sarma, H. P. (2012). Heavy metal contaminations in the groundwater of Brahmaputra flood plain: an assessment of water quality in Barpeta District, Assam (India). *Environmental Monitoring and Assessment, 184*(10), 6229–6237.

Hernandez, L., Probst, A., Probst, J. L., et al. (2003). Heavy metal distribution in some French forest soils: evidence for atmospheric contamination. *Science of the Total Environment, 312*(1–3), 195–219.

Horneman, A., Van Geen, A., Kent, D. V., et al. (2004). Decoupling of As and Fe release to Bangladesh groundwater under reducing conditions. Part 1: Evidence from sediment profiles. *Geochimica et Cosmochimica Acta, 68*(17), 3459–3473.

Huntsman-Mapila, P., Kampunzu, A. B., Vink, B., et al. (2005). Cryptic indicators of provenance from the geochemistry of the Okavango Delta sediments, Botswana. *Sedimentary Geology, 174*(1–2), 123–148.

Islam, F. S., Gault, A. G., Boothman, C., et al. (2004). Role of metal-reducing bacteria in arsenic release from Bengal delta sediments. *Nature, 430*(6995), 68–71.

Lee, S. S., Lim, J. E., Abd El-Azeem, S. A. M., et al. (2013). Heavy metal immobilization in soil near abandoned mines using eggshell waste and rapeseed residue. *Environmental Science and Pollution Research, 20*(3), 1719–1726.

Li, J., Peng, F. L., Ding, D. B., et al. (2011). Characteristics of the phytoplankton community and bioaccumulation of heavy metals during algal blooms in Xiangjiang River (Hunan, China). *Science China-Life Sciences, 54*(10), 931–938.

Li, G., Tong, F. P., & Liu, Z. H. (2012). Analysis on pollution of heavy metal in Shuikoushan Pb-Zn mining and smelting area in Hengyang. *Journal of Central South University of Forestry & Technology, 32*(7), 105–109.

Lian, S. T., & Xiao, J. (2010). Analysis on the environment background values of groundwater from Dongting Lake, *Fujian Architecture & Construction (in Chinese)* (10), 61–63.

Ma, L. Y., Lu, Y. F., Me, Y. P., et al. (2006). Zircon SHRIMP U-Pb dating of granodiorite from Shuikoushan ore-field, Hunan Province and its geological significance. *Acta Petrologica Sinica, 22*(10), 2475–2482.

Maharia, R. S., Dutta, R. K., Acharya, R., et al. (2010). Heavy metal bioaccumulation in selected medicinal plants collected from Khetri copper mines and comparison with those collected from fertile soil in Haridwar, India. *Journal of Environmental Science and Health Part B: Pesticides Food Contaminants and Agricultural Wastes, 45*(2), 174–181.

McMurtry, G. M., Wiltshire, J. C., & Kauahikaua, J. P. (1995). Heavy metal anomalies in coastal sediments of Oahu, Hawaii. *Pacific Science, 49*(4), 452–470.

Mok, W. M., Riley, J. A., & Wai, C. M. (1988). Arsenic speciation and quality of groundwater in a lead zinc mine, Idaho. *Water Research, 22*(6), 769–774.

Murphy, E. M., & Zachara, J. M. (1995). The role of sorbed humic substances on the distribution of organic and inorganic contaminants in groundwater. *Geoderma, 67*(1–2), 103–124.

Namaghi, H. H., Karami, G. H., & Saadat, S. (2011). A study on chemical properties of groundwater and soil in ophiolitic rocks in Firuzabad, east of Shahrood, Iran: with emphasis to heavy metal contamination. *Environmental Monitoring and Assessment, 174*(1–4), 573–583.

Oremland, R. S., & Stolz, J. F. (2003). The ecology of arsenic. *Science, 300*(5621), 939–944.

Panda, U. C., Rath, P., Bramha, S., et al. (2010). Application of factor analysis in geochemical speciation of heavy metals in the sediments of a Lake System-Chilika (India): a case study. *Journal of Coastal Research, 26*(5), 860–868.

Park, J. H., & Choi, K. K. (2013). Risk assessment of the abandoned Jukjeon metal mine in South Korea following the Korean guidelines. *Human and Ecological Risk Assessment, 19*(3), 754–766.

Park, S., & Lee, B. K. (2013). Body fat percentage and hemoglobin levels are related to blood lead, cadmium, and mercury concentrations in a Korean adult population (KNHANES 2008–2010). *Biological Trace Element Research, 151*(3), 315–323.

Qiao, Y. M., Yang, Y., Gu, J. G., et al. (2013). Distribution and geochemical speciation of heavy metals in sediments from coastal area suffered rapid urbanization, a case study of Shantou Bay, China. *Marine Pollution Bulletin, 68*(1–2), 140–146.

Rai, P. K. (2010). Heavy metal pollution in lentic ecosystem of sub-tropical industrial region and its phytoremediation. *International Journal of Phytoremediation, 12*(3), 226–242.

Salvarredy-Aranguren, M. M., Probst, A., Roulet, M., et al. (2008). Contamination of surface waters by mining wastes in the Milluni Valley (Cordillera Real, Bolivia): mineralogical and hydrological influences. *Applied Geochemistry, 23*(5), 1299–1324.

Schiff, K. C., & Weisberg, S. B. (1999). Iron as a reference element for determining trace metal enrichment in southern California coastal shelf sediments. *Marine Environmental Research, 48*(2), 161–176.

SEPA (2002). The monitoring and analysis method of water and wastewater (4th ed.).

SEPA (2007). Solid waste-extraction procedure for leaching toxicity-sulfuric acid and nitric method (HJ/T299-2007).

Sun, G. X., Wang, X. J., & Hu, Q. H. (2011a). Using stable lead isotopes to trace heavy metal contamination sources in sediments of Xiangjiang and Lishui Rivers in China. *Environmental Pollution, 159*(12), 3406–3410.

Sun, Y., Shu, F., Hao, W., et al. (2011b). Heavy metal contamination and Pb isotopic composition in natural soils around a Pb/Zn mining and smelting area. *Chinese Journal of Environmental Science, 32*(4), 1146–1153.

Sun, W. L., Sang, L. X., & Jiang, B. F. (2012a). Trace metals in sediments and aquatic plants from the Xiangjiang River, China. *Journal of Soils and Sediments, 12*(10), 1649–1657.

Sun, X., Ning, P., Tang, X. L., et al. (2012b). Heavy metals migration in soil in tailing dam region of Shuikoushan, Hunan Province, China. *Seventh International Conference on Waste Management and Technology (Icwmt 7), 16*, 758–763.

Sutherland, R. A. (2000). Bed sediment-associated trace metals in an urban stream, Oahu, Hawaii. *Environmental Geology, 39*(6), 611–627.

Tan, J. X., & Wang, K. Y. (2008). Geochemical characteristics of Shuikoushan lead-zinc-gold-silver deposit, Hunan Province. *Geology and Prospecting, 44*(3), 6.

Toth, J. (1999). Groundwater as a geologic agent: an overview of the causes, processes, and manifestations. *Hydrogeology Journal, 7*(1), 1–14.

Tufano, K. J., Reyes, C., Saltikov, C. W., et al. (2008). Reductive processes controlling arsenic retention: revealing the relative importance of iron and arsenic reduction. *Environmental Science & Technology, 42*(22), 8283–8289.

Van Geen, A., Rose, J., Thoral, S., et al. (2004). Decoupling of As and Fe release to Bangladesh groundwater under reducing conditions. Part II: Evidence from sediment incubations. *Geochimica et Cosmochimica Acta, 68*(17), 3475–3486.

Wang, L. X., Guo, Z. H., Xiao, X. Y., et al. (2008). Heavy metal pollution of soils and vegetables in the midstream and downstream of the Xiangjiang River, Hunan Province. *Journal of Geographical Sciences, 18*(3), 353–362.

Wei, C. Y., Wang, C., & Yang, L. S. (2009). Characterizing spatial distribution and sources of heavy metals in the soils from mining-smelting activities in Shuikoushan, Hunan Province, China. *Journal of Environmental Sciences-China, 21*(9), 1230–1236.

WHO (2011). Guidelines for drinking-water quality (4th ed.), annex 3.

Zamani, A. A., Yaftian, M. R., & Parizanganeh, A. (2012). Multivariate statistical assessment of heavy metal pollution sources of groundwater around a lead and zinc plant. *Iranian Journal of Environmental Health Science & Engineering, 9*.

Zeng, N. S., Izawa, E., Motomura, Y., et al. (2000). Silver minerals and paragenesis in the Kangjiawan Pb-Zn-Ag-Au deposit of the Shuikoushan mineral district, Hunan Province, China. *Canadian Mineralogist, 38*, 11–22.

Zhang, L. C., & Zhao, G. J. (1996). The species and geochemical characteristics of heavy metals in the sediments of Kangjiaxi River in the Shuikoushan Mine Area, China. *Applied Geochemistry, 11*(1–2), 217–222.

Zhang, Z., Tao, F. L., Du, J. A., et al. (2010). Surface water quality and its control in a river with intensive human impacts—a case study of the Xiangjiang River, China. *Journal of Environmental Management, 91*(12), 2483–2490.

Zhang, T., Zhang, Y., Li, D. L., et al. (2013). Exposure of silver carp (Hypophthalmichthys molitrix) to environmentally relevant levels of cadmium: hematology, muscle physiology, and implications for stock enhancement in the Xiangjiang River (Hunan, China). *Science China-Life Sciences, 56*(1), 66–72.

Zobrist, J., Sima, M., Dogaru, D., et al. (2009). Environmental and socioeconomic assessment of impacts by mining activities-a case study in the Certej River catchment, Western Carpathians, Romania. *Environmental Science and Pollution Research, 16*, 14–26.